Digest Journal of Nanomaterials and Biostructures, Vol. 2, No. 4, December 2007, p. 315- 333

ATOMIC CLUSTERS AND NANOSTRUCTURES

L. C. Cune, M. Apostol

Department of Theoretical Physics, National Institute of Physics and Nuclear Engineering, Bucharest-Magurele, P. O. Box Mg-35, Romania

The quasi-classical theoretical description of matter aggregation and solid-state cohesion at atomic level is briefly presented in connection with its multiple applications to atomic clusters and nanostructures. The formation of isolated atomic clusters of up to 160 atoms is presented and characterized with respect to geometric forms, atomic positions, inter-atomic distances, ground-states and isomers, binding energies, magic numbers, vibration spectra, and the derivation of single-particle properties is outlined, within the point-like ions approximation. The surface of a semi-infinite solid is characterized within the same approach, and the formation of clusters deposited on surfaces is described, with regard to similar physical and chemical information. Peculiar nanostructures are also presented, as resulted from computation processes, as an indication of the large variety of possible nanostructured forms. The extension of the theoretical tools to more complex situations, in particular to directional bonds and quantum corrections, is also discussed.

(Received December 24, 2007; accepted December 28, 2007)

Keywords: Cluster, Nanostructure, Matter aggregation, Surface supported clusters, Computing calculation, Point like ion approximation

1. Introduction

The tremendous upsurge of activity in nanotechnologies witnessed at present raises basic issues of matter aggregation and structuration at the atomic level. While enabling major breakthroughs in life sciences and medicine, ultraminiatural electronics, materials, tools and processes, and manipulating individual atoms at the same time, the nanoscale sciences provide a more direct, sensible representation of the atomic and molecular matter, together with a more accurate knowledge of the physical and chemical structures and processes at this level. Traditionally, the field bears relevance upon chemical bonding of molecules and solid-state bulk bodies. However, in-between there is an extremely large amount of various kinds of supramolecules, molecular aggregates, atomic clusters, nanostructures and nano-objects, either isolated or in various environments, sometime exhibiting intricate geometries and beautiful symmetries, with their own specific behaviour. This immense new realm that fills plenty in the ”room at the bottom” displays basically a quantum behaviour and size dependence. These issues are addressed in the present paper, from the perspective of the quasi-classical description of assemblies of valence electrons and charge-compensating point like ionic cores, with particular emphasis on relevant physical and chemical information on various atomic clusters and nanostructures, both isolated or under various geometric constraints as, for instance, clusters deposited on surfaces. In particular, geometric forms, atomic positions, interatomic distances, binding energies, magic numbers and vibration spectra are presented, and the extension to single-particle properties and structured ionic cores is outlined. Within given approximation, the results are applicable to homo-atomic metallic formations.

2. Theoretical

In chemical binding the single-electron wave functions are superpositions of localized atomic-like orbitals and extended bond-like orbitals. Due to the great disparity in the spatial scales of the two types of orbital the problem of the nuclei-electrons interaction is separated into a purely atomic like part, a chemical-bond part, and a residual interaction, which can further be removed by using classical variation principles [1]. The atomic-like part can be treated by standard ab-initio wave functions method [2], while for the chemical-bond part a quasi-classical description has been

developed recently [3], in close connection with the density-functional method [4]. For the chemical bond part we are left with an ensemble of electrons moving in a background of neutralizing effective charges in the valence upper shells of the ions. These charges are distributed in space according to the corresponding atomic-like orbitals, but we adopt here, for the sake of the simplicity, a point-like distribution

$$\rho(\mathbf{r}) = \sum_{i=1}^{N} z_i^* \delta(\mathbf{r} - \mathbf{R}_i) \quad , \tag{1}$$

where z^*_i are the effective charges (in units of electron charge e) and $\mathbf{R}_i$ denote the positions of N ions, i = 1, 2, ...N . Such a point-like ionic charge distribution bears a limited relevance upon certain s-, d- and f-metallic ions, where we may neglect the radial dependence of the atomic like orbitals and average out their angular dependence, but it is inadequate for an important, very large class of ions with p-valence orbitals, or with hybridized valence orbitals. The effective charges can, in principle, be obtained by solving the entire problem of nuclei-electrons interaction, as remarked above, but results are not yet available. However, for certain ions, within the point-like approximation, we may estimate the effective charges by making use of the atomic screening theory [5]. For instance, we get $z^* = 0.57$ for Fe^{2+}(iron), $z^* = 0.34$ for Ba^{2+}(barium), and $z^* = 0.44$ for Na^+ (sodium). Such estimations, together with the point-like approximation, render a status of model-calculations to the results presented herein. In addition, the theoretical treatment employed here is valid for a suffciently large number N of not-too-light atoms.

Within the quasi-classical description of the Hartree-Fock equations [3] the chemical-bond orbitals are quasi-plane waves in the first approximation, and the electrons move in the Hartree selfconsistent field

$$\varphi(\mathbf{r}) = \sum_{i=1}^{N} \frac{z_i^*}{|\mathbf{r} - \mathbf{R}_i|} e^{-q|\mathbf{r}-\mathbf{R}_i|} \tag{2}$$

corresponding to the charge distribution given by (1), where q is a screening wave vector similar to the Thomas-Fermi wave vector, to be determined variationally. The self-consistency requires a linear relationship $n = (q2/4\pi)\varphi$ between the electron density n and the potential φ, which allows a straightforward computation of the interaction energy. This energy includes the Coulomb attraction between electrons and ions and the Coulomb repulsions both between electrons and between ions, respectively. We call it potential energy, and it is given by

$$E_{pot} = -\frac{3}{4} q \sum_{i=1}^{N} z_i^{*2} + \frac{1}{2} \sum_{i \neq j=1}^{N} \Phi(R_{ij}) \quad , \tag{3}$$

where

$$\Phi(R_{ij}) = -\frac{1}{2} q z_i^* z_j^* (1 - \frac{2}{qR_{ij}}) e^{-qR_{ij}} \tag{4}$$

is the effective (pseudo-) potential acting between two ions separated by the distance $R_{ij} = |R_i - R_j|$. This inter-ionic potential is shown in Figs. 1 and 2. It has an attractive tail at long distances and is strongly repulsive at short distances.

The interacting part in E_{pot} is the only contribution which depends on the ionic positions, so that we may minimize this energy represented by the second term in the r.h.s. of (3) with respect to $\mathbf{R}_i$ (actually with respect to the dimensionless variables $\mathbf{X}_i = q\mathbf{R}_i$) in order to get the equilibrium forms of the ensemble of ions; doing so, we get both the ground-state of the ionic aggregate and the isomers, which differ by slight changes in energy and ionic positions. They correspond to local minima of the potential energy (3). The minimum values of the interacting part in (3) is usually very small in comparison with the self-energy ionic part given by the first term in the r.h.s. of (3), so we may neglect this contribution in approximate estimations. The model of metal obtained here resembles very much the ancient Wigner-Seitz model [6].

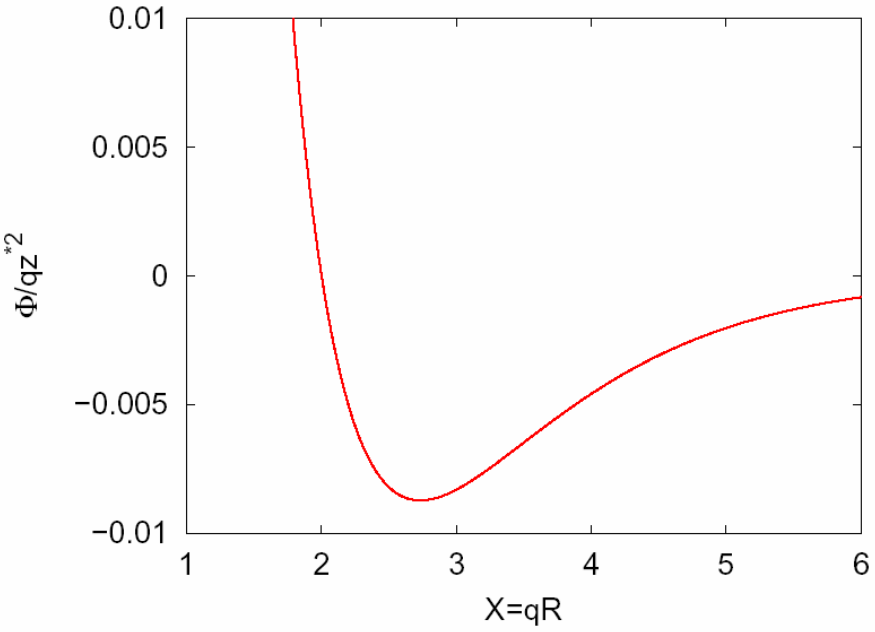

Figure 1: The inter-ionic potential function *vs* reduced distance

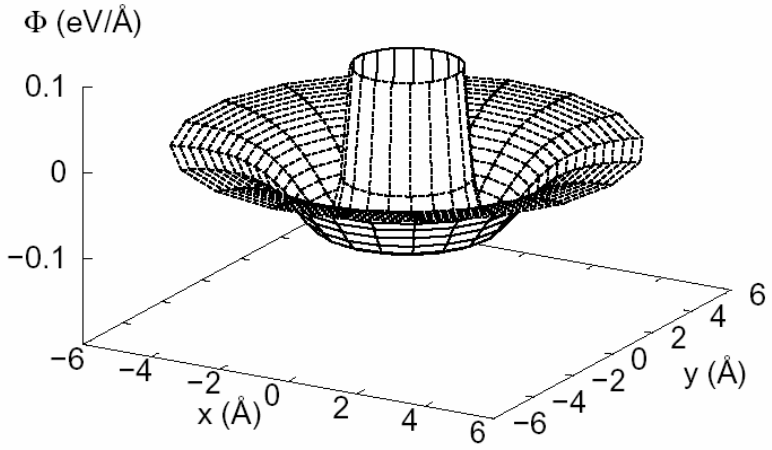

Figure 2: A two-dimensional sheet of the inter-ionic potential (4) for Fe-ions

The quasi-classical description is based upon slight spatial variations of the electron density in extended chemical-bonds orbitals; this enables the linear self-consistency relationship given above between electron density and potential. Accordingly, such a linearization is in order for the kinetic energy of the electrons too; it reads[1] $E_{kin} = (27\pi^2/640)q^4\Sigma_i\, z^*_i$. The quasi-classical energy $E_q = E_{kin} + E_{pot}$ is then obtained, where E_{pot} is the ground-state minimum value of the potential energy (3), and minimized with respect to the screening wave vector q. It is easy to see that such a

minimum value exists; for homo-atomic aggregates it is given by $q \approx 0.77 z^{*1/3}$, neglecting the small contribution of the interacting part to the potential energy at equilibrium. In this case we may also define an average inter-ionic distance a by $aq \approx 2.73$, where $X = 2.73$ is the reduced distance where the inter-ionic potential (4) reaches its minimum value.

The exchange energy in the Hartree-Fock equations admits plane waves as eigenstates. More, it remains unchanged for quasi-plane waves, i.e. for slight local changes in the electron density, as in the quasi-classical description, due to its non-local character[2]; it follows that screening does not a_ect it in this approximation, so we may simply add its (linearized) contribution $E_{ex} = -(9/32) q^2 \Sigma_i z^*_i$ to the quasi-classical energy Eq, with q determined above, to obtain the binding energy $E = Eq + E_{ex}$. For homo-atomic aggregates the ground-state energy is given by $E = (0.43 z^{*7/3} + 0.17 z^{*5/3})$, leaving aside the small contribution of the interacting part of (3) (which however is responsible for the non-thermodynamic behaviour and the size dependence).

The theoretical scheme outlined above is a linearized Thomas-Fermi model in fact, as derived from the quasi-classical solution of the Hartree-Fock equations. It differs from the standard non-linear Thomas-Fermi model (characterized by $n \sim \varphi^{3/2}$) in that it exhibits binding of the interacting ions and electrons, in contrast to the latter where there is no binding.[8] The non-linear Thomas-Fermi model is valid in the limit of infinite ionic charges (so-called quasi-classical limit), while the linearized model presented here is the starting point of the quantum behaviour of matter aggregation, and it could represent the solution to chemical bonding Schwinger was alluding to [9]. It has been applied to heavy atoms (with atomic numbers $Z \gg 1$) where the well-known binding energy $-16 Z^{7/3}$eV has been successfully reproduced (quantum corrections included), to a consistent analysis of bulk properties of a model of "universal" metal, and to realistic estimations of the ionization potentials of metallic clusters [10]. The quasi-classical description as presented above is only the first step in a full treatment. It offers the great advantage of getting structured atomic ensembles with rather limited computational resources. On the other hand, it offers the possibility of pursuing consistently the so-called quantum corrections. The latter include the ab-initio computation of the effective charge parameters as indicated before, taking into account the entire problem of nuclei-electrons interaction, as well as the single-particle properties, in particular the single-electron energy levels of the electrons motion in the self-consistent potential φ, as given by (2), for instance [3]. These corrections bring certain changes in energies and, consequently, equilibrium ionic positions, as well as other relevant quantities. The quantum corrections are basically due to the strong variations of the electron density and self-consistent potential over small distances of the order of atomic distances. These deviations can be estimated, if one considers, for instance, the screening wave vector q as related to the average of the Fermi wave vector; doing so we obtain ~ 17 % an accuracy of the quasi-classical results. Further on, the single-particle wave functions of the Hartree-Fock equations entail an inherent second-order uncertainty in the self-consistency scheme, which signals its limits; therefore, we conclude that, once the quantum corrections included, the results are valid within at most $\sim 0.17 \times 17\ \% \approx 3\ \%$ accuracy, and this would be the limit of the approach.

---

[1] In atomic units e^2/a_H _= 27.2eV, where $a_H = \hbar^2/me^2 \approx 0.53$ Å is the Bohr radius (m is the electron mass and $\hbar$ denotes the Planck constant).

[2] This "rigidity" character of the exchange energy has been noticed probably for the first time by Slater [7] (see also Ref. [6]).

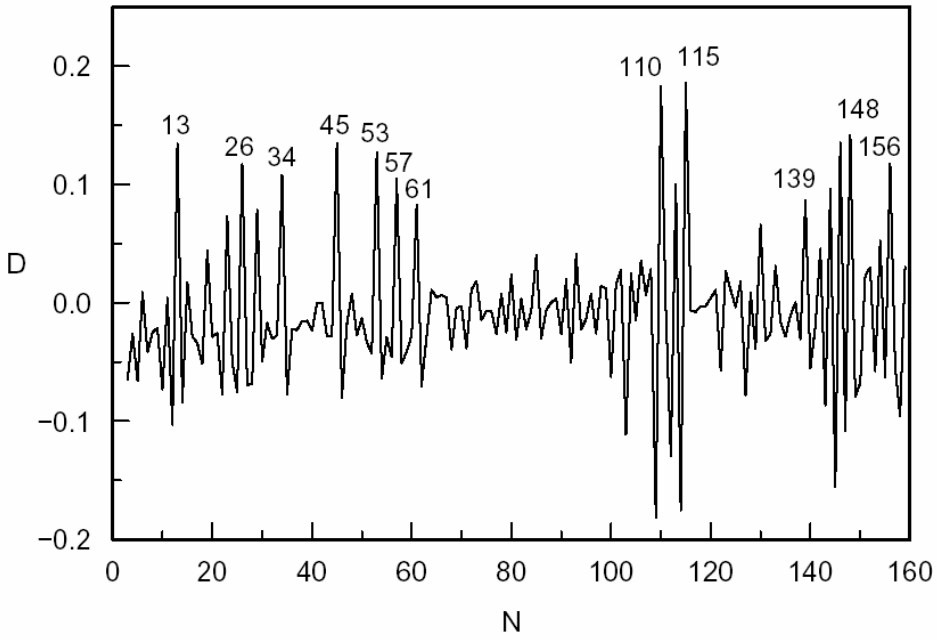

Figure 3 Ground-state mass spectrum of metallic clusters

3. Metallic Clusters

The first step in applying the method described above is to minimize the potential energy given by (3) and (4) with respect to the reduced ionic positions $\mathbf{X}_i = q\mathbf{R}_i$. Since the X-dependence of the potential function Φ does not involve the nature of the ions, the equilibrium geometric forms found by such a minimization are universal. The minimization method is implemented by giving originally ionic positions randomly distributed in space, computing the forces at each position, and letting the ions move step by step in the direction of the forces, until an equilibrium is reached (actually until the forces are less than 10^{-4}eV/Å). The equilibrium positions can correspond either to the ground-state or to isomers. In order to distinguish the ground-state from the isomers we run several hundreds times the equilibrium process for each atomic aggregate, attempting to get a statistical ensemble as large as possible. In addition, for differentiating between local minima and saddle-points we compute also the vibration spectra in the harmonic-oscillator approximation. Finally, we compute the quasi-classical energy E_q, find out its minimum value and the screening wave vector q, add the exchange energy E_{ex} and get the binding energy E for the ground-state, as described in Section 2. The latter exhibits small, irregular variations with respect to the number N of atoms; to put them clearly into evidence we compute also the so-called abundance, or mass spectrum, as given by $D = \ln(I_N^2/I_{N+1}I_{N-1}) = E(N + 1) + E(N - 1) - 2E(N)$, where I_N is the Boltzmann statistical weight for the ground-state. It is found that such a spectrum does not depend on the effective charges z^* within reasonably large limits. This procedure has been applied to homo-atomic clusters of metallic ions up to N = 160.

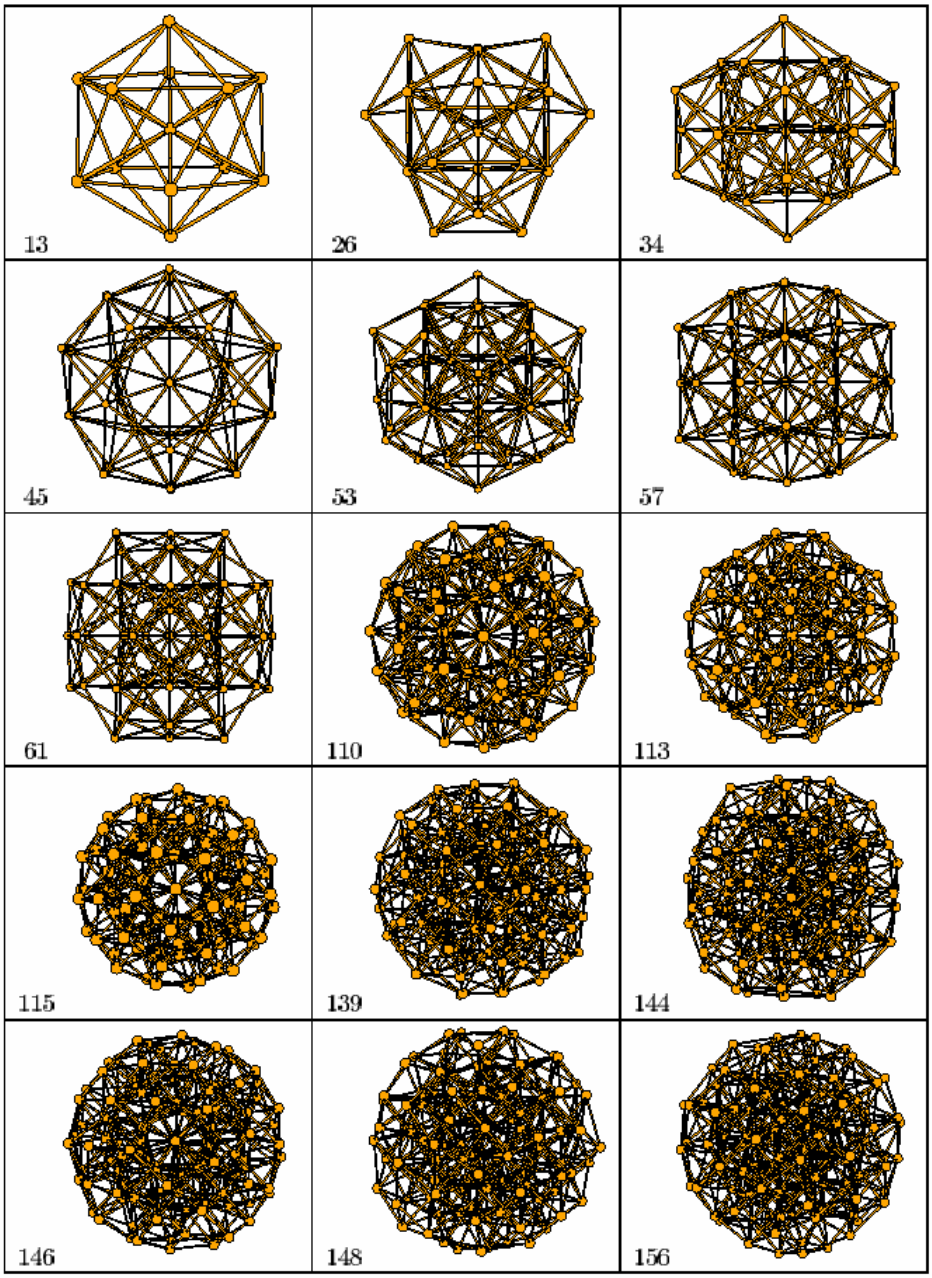

Figure 4: Magic clusters of metallic ions

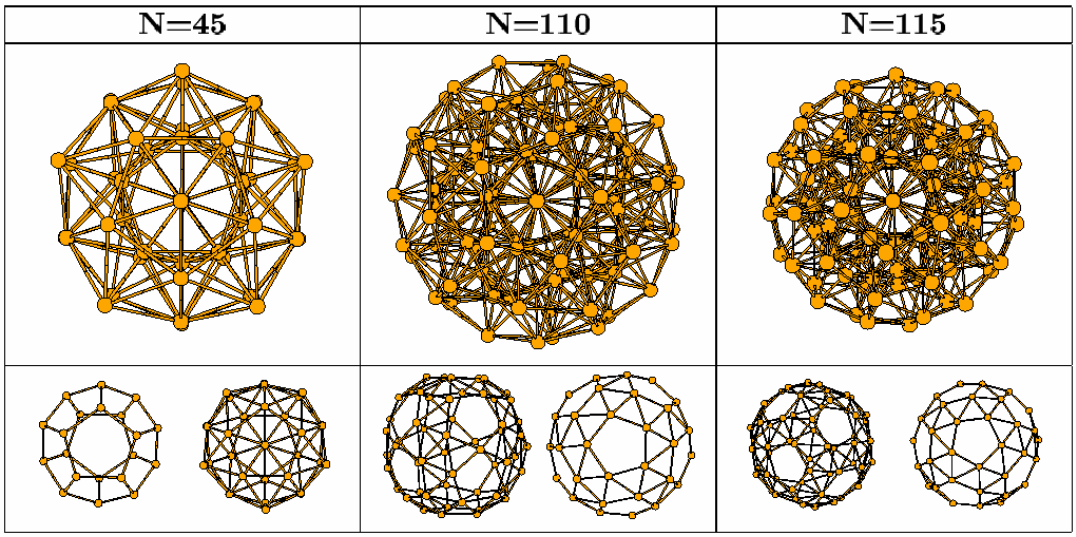

Figure 5 Highly symmetric metallic clusters (first row), displaying outer shells (second row).

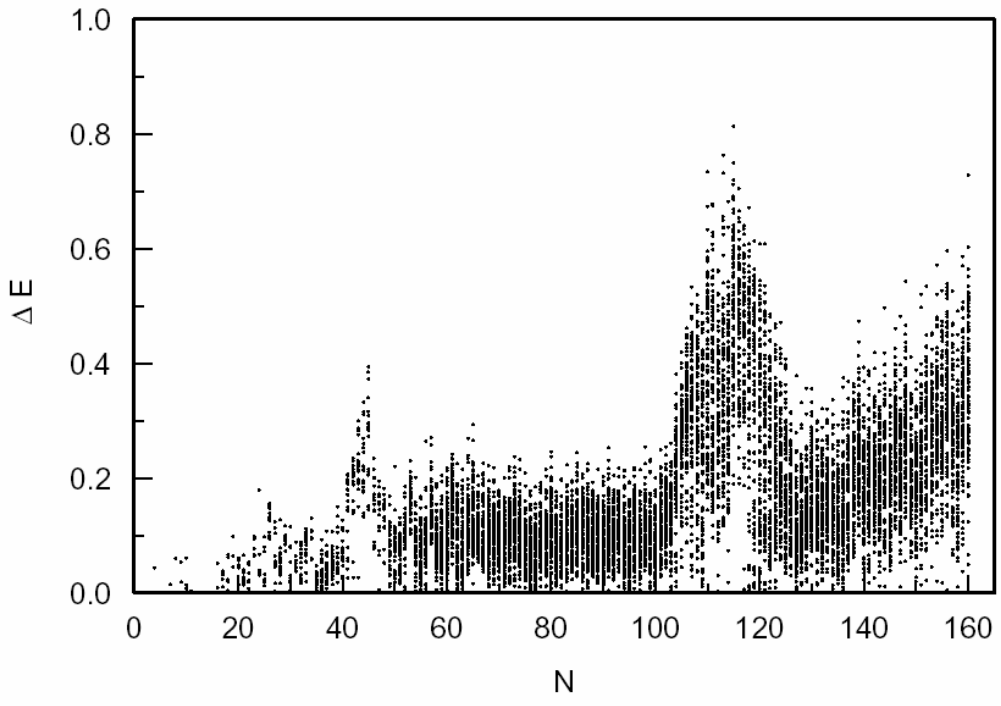

Figure 6: Isomer table of Fe-clusters

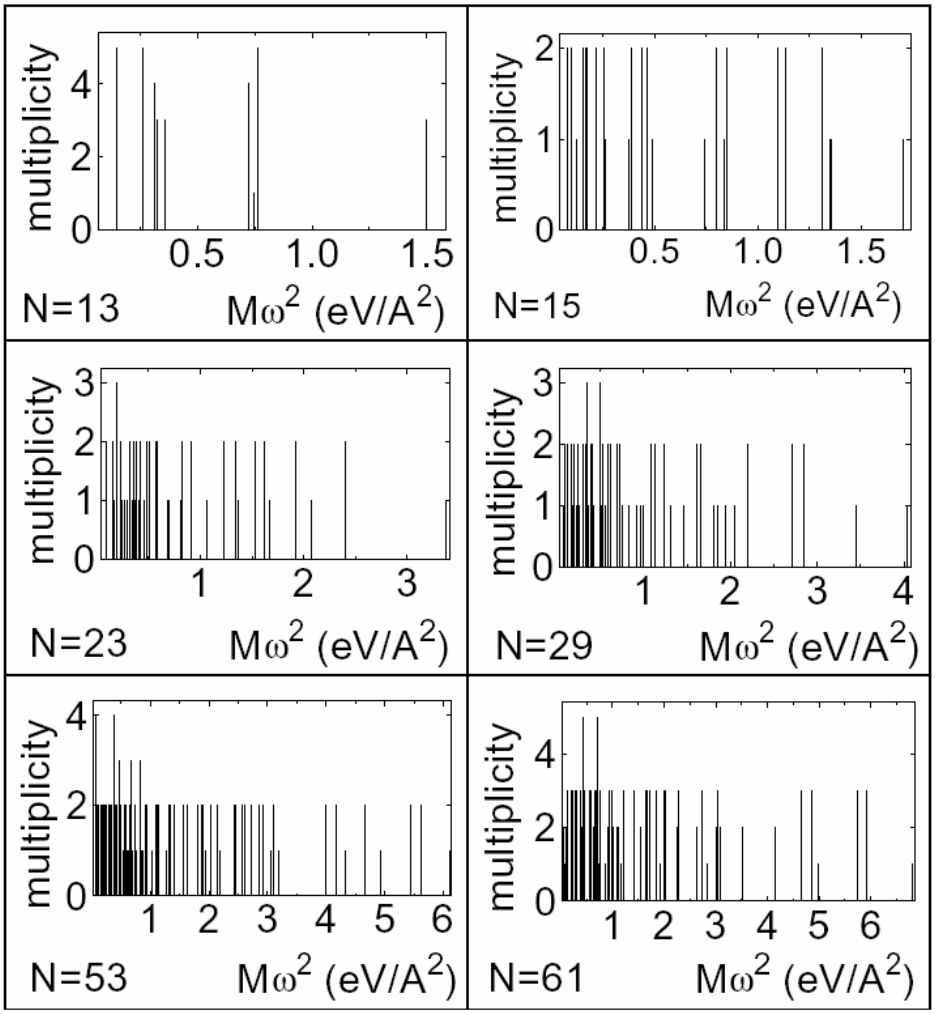

Figure 7 Ground-state vibration spectra of ground-state Fe-clusters.

The mass spectrum of homo-atomic metallic clusters is shown in Fig. 3. It exhibits a sequence of high and very sharp peaks, corresponding to what we call magic clusters. Indeed, these magic clusters in their ground-states are much more stable as compared to their neighbours, and may possess a high symmetry, most of them a pentagonal one, like the centered icosahedron N = 13.

Some of these magic clusters are shown in Fig. 4. For relatively small values of N we expect to get Plato's perfect polyhedra. However, this is not always true. For instance, we obtain the tetrahedron (N = 4) and the octahedron (N = 6), but the hexahedron (cube, N = 8) and the dodecahedron (N = 20) are not ground-states (we get them as isomers), while the icosahedron prefers to be centered (N = 13). It seems that the principle of atomic packing in such magic clusters is a certain "space economy". Indeed, this can be shown convincingly on the three "most magic" clusters shown in Fig. 5, with N = 45, 110 and 115, respectively. The first row in Fig. 5 shows a front view which displays the highly symmetric forms of these clusters, while their outer shells are shown in the second row; indeed, such clusters are made of multiple, closed geometric E(N)/N (eV) atomic shells, with one shell's atoms placed just above the facets' centers of another.

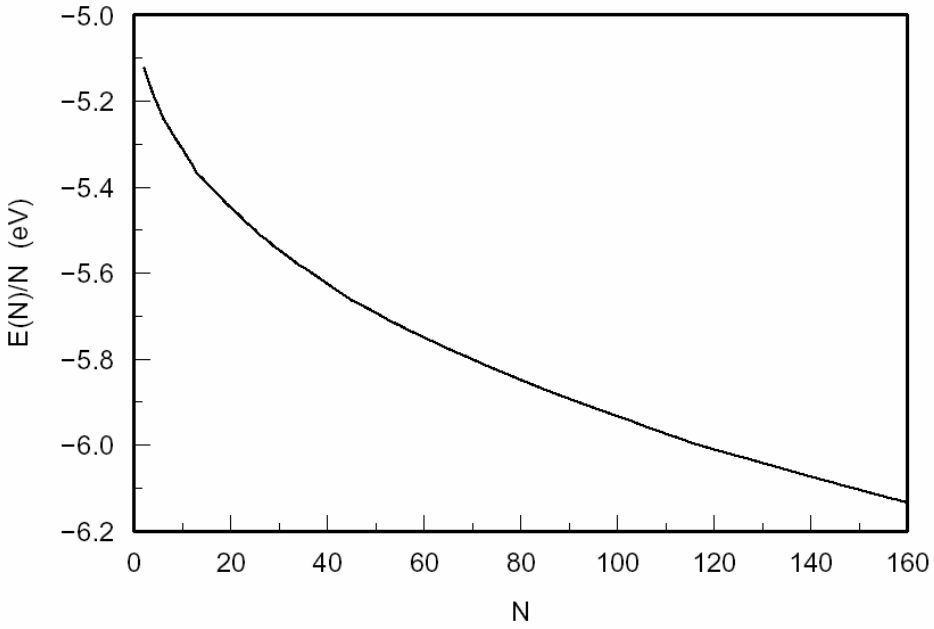

Figure 8 Ground-state energy per atom of Fe-clusters bs cluster size.

These clusters display an outstanding five-fold symmetry, yet other magic clusters, though very close to a high symmetry, exhibits also slight, disconcerting imperfections, like the N = 113, 144, or 148 clusters in Fig. 4. It is worth noting here that some of these structures have also been obtained either by other theoretical techniques, or have been identified experimentally [11], and the five-fold symmetry magic numbers like N = 13, 45, 115 are known as geometric, or icosahedral magic numbers. As regarding a possible comparison with experimental results a word of caution is in order here. First, it must be stressed that the mass spectrum given in Fig. 3 corresponds to the ground-states, while clusters are usually produced experimentally in a statistical ensemble at a non-vanishing temperature.

Consequently, a statistical average is relevant for experimental abundance, which includes isomers beside the ground-state; this gives ”statistical”magic numbers N, as distinct from the present ”geometric”, or ”ground-state” magic numbers given in Fig. 3. A table of isomers is given in Fig. 6 for Fe-clusters, where we may notice an increase in the number of isomers on increasing size, as well as several ”white islands” placed approximately at the magic clusters (for instance at N = 13, 45 and 115), as expected. Similarly, it is worth noting that slight differences in energy differentiate the isomers from the ground-states. Secondly, ”electronic” magic numbers may be obtained, as different from the two previous ones, from the filling up of the electron states in model potentials, like the well-known quadropole-deformed harmonic-oscillator potential. In particular, the latter potential is obtained from the self-consistent potential (2) in the long-wavelengths (continuum) limit [3], which may be relevant for other sets of experimental data, depending on the clusters nature and the particular conditions of producing these clusters.

Having obtained the equilibrium ionic coordinates $\mathbf{X}_i$ by minimization of the potential energy, and the screening wave vector q from the minimum value of the quasi-classical energy, we may obtain the inter-ionic distances $R_{ij} = X_{ij}/q$ at equilibrium; on the average they are of the order of 2-3 Å . It is worth noting that for computing such quantities, as well as for computing the binding energy or the vibration spectra, one needs to know the nature of the atomic species, in particular the

effective charges z*. The vibration spectra for several magic clusters of Fe in the ground state are

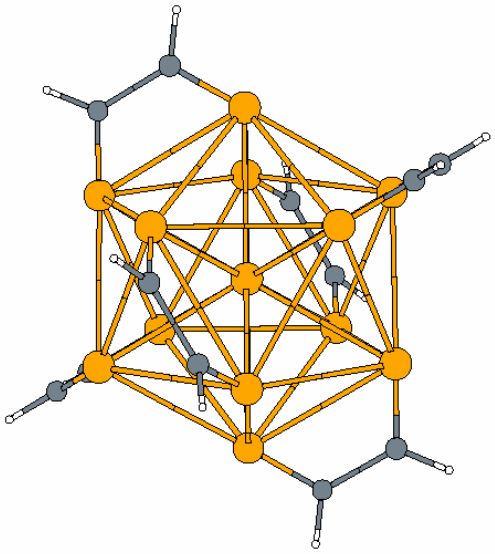

Figure 9 A $Fe_{13}(C_2H_2)_6$ cluster (Ref. 14, 15).

shown in Fig. 7. One can notice the increase of low-energy vibration states density with increasing cluster size, as expected, as well as higher multiplicity of the vibration states for more symmetric clusters. The binding energy per atom for the ground state of Fe-clusters (z* = 0.57) is given in Fig. 8 vs cluster size N. The binding energies of such clusters are of the order of 5 - 6 eV per atom. These numerical values are in good agreement with the results of other computations [12]. In this respect, it is worth mentioning the large amount of work devoted to metallic clusters, by employing both *ab-initio* calculations, molecular dynamics, density functionals, or jellium-like models. Numerical data, when available, can be found, for instance, in Ref. 13.

The results presented here suggest that metallic clusters produced experimentally by various techniques may have very likely equilibrium geometric forms like those given in Fig. 4 for their ground-states or slightly different ones for their isomers. Most metallic clusters serve as cores for more complex, nanostructured aggregates, like organo-metallic clusters (as we shall see in the next section), and the core geometry brings useful information in designing the structure and the functionality of the latter. The presence of the isomers, which are separated from the ground-state by small amounts of energy, is particularly interesting in giving indication about cluster stability and their possible tunneling between various geometric configurations. A privileged position in this connection has the magic clusters associated with ”white islands” in the isomer table in Fig. 6, but the origin of the rather wide energy gaps between the ground-state and the first excited state in this case is not known; at most, we can trace it back to a rather vague principle of ”space economy”, as said above.

4. Peculiar nanostructures

The theoretical model of atomic aggregation presented in Section 2 can also be applied to more complex clusters. Such a complex organic-metallic cluster is the iron-hydrocarbonated $Fe_{13}(C_2H_2)_6$ which has recently been synthesized experimentally [14]. Since each CH-radical may

bind to a Fe ion by taking one valence electron, it seems naturally to assume that 12 Fe-ions possess

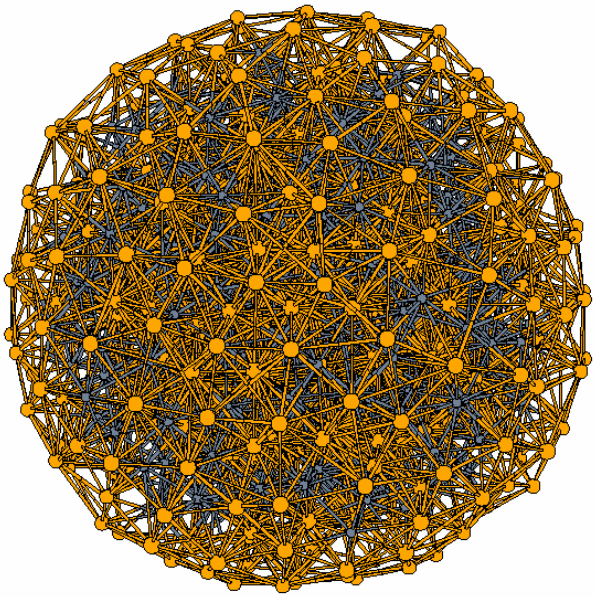

Figure 10: An 855-atoms bit of metal

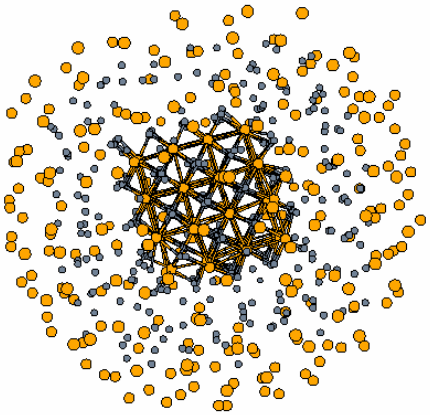

Figure 11: A *bcc*-core of an 855-atoms metal

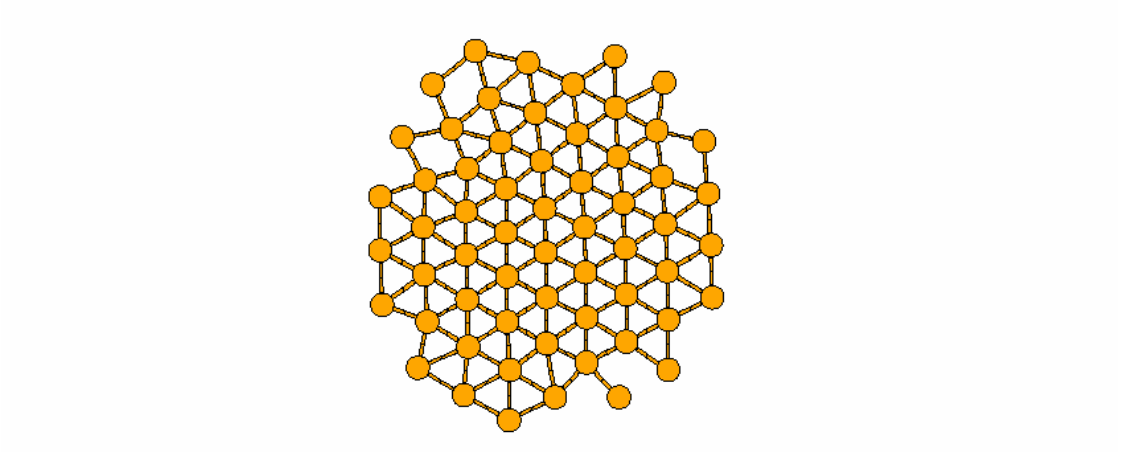

Figure 12 An unstable hexagonal metallic sheet

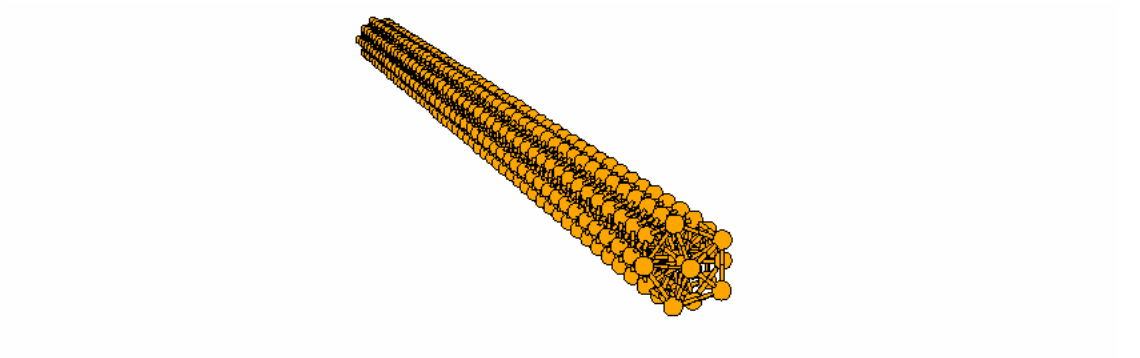

Figure 13 A metallic popcorn wire (unstable).

half of the effective charge of a standard Fe-ion, i.e. z* = 0.57/2 = 0.28, and view the entire structure as consisting of 12 such Fe-CH ions and one standard Fe-ion (with effective charge z* = 0.57).

Such a structure clusterizes into a centered perfect icosahedron as the one shown in Fig. 5 for N = 13, which may be viewed as the core of the actual organic-metallic cluster $Fe_{13}(C_2H_2)_6$. Simple arguments of a minimal interaction energy between the C_2H_2-acetylene radicals lead then to a symmetric arrangement of them on the surface of the Fe-core cluster, as shown in Fig. 9. The contribution of the metallic core to the binding energy has been estimated, as well as the interatomic distances, vibration spectrum and the electron charge distribution [15] getting thus useful preliminary information for a more detailed study, which must include the directional bonding of the C_2H_2- radicals.

A more complex experiment has been run on computer by making use of the present theory. It consists of giving 83-unit cells of a bcc-metal and let the ions relax to equilibrium. Doing so, a huge cluster of N = 855 atoms has been obtained as shown in Fig.10, with a pretty disordered structure, which however preserves an approximate original bcc-symmetry in a core of about 3 unit cells, as shown in Fig. 11. The computations take a rather long time in this case, and the statistics of the results is poor enough to have a reliable structure. However, this may give useful indications as to how the translation symmetry of a bulk solid may appear on increasing the number of atoms, and the extent of the surface (finite-size) effects. It has also found that the isomers of such a chunk of solid are extremely numerous, within a narrow energy range just above the ground-state energy, as expected, but, what is very interesting, they are associated mainly with slight, multiple changes in the positions of the outer ions. It suggests that the surface of a very large cluster, or of a solid, might be fuzzy, as corresponding to a superposition of states with slightly different atomic positions, very similar to a liquid (it may be termed a ”quasi-liquid”).

In some computer runnings various peculiar nanostructures have been obtained accidentally,

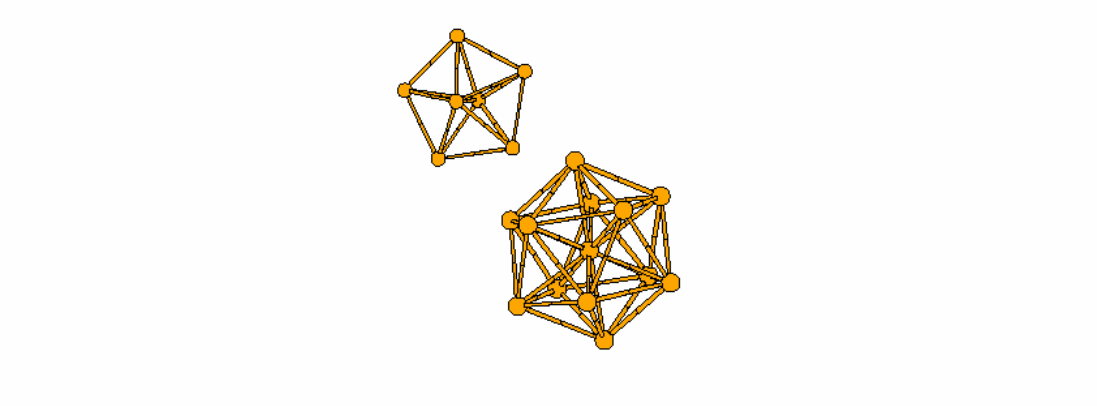

Figure 14 Two weakly interacting metallic clusters

each with suggestive particularities. For instance, we got an atomic sheet with an almost perfect hexagonal symmetry, as shown in Fig. 12, which is unstable, as expected (it may be stabilized by depositing it on a surface); or unstable chains of metallic ions, the most interesting being the one shown in Fig. 13. It consists of a sequence of inter-twined, mutually rotated icosahedra, leaving outside one protruding icosahedral end-atom, which might be suggestive for a perfect probe tip in scanning microscopy. The chain is however unstable, as expected for such a simplified one-dimensional model of metal, but its diameter is smaller than the inner diameter of a carbon nanotube, so the latter may act as a stabilizing support. The results obtained within the present theoretical approach for such low-dimensional nanostructures, beside their suggestive character, may be useful as a constitutive input for more elaborate theoretical models.

Another very interesting situation appeared in a few computer runnings where a number of metallic ions aggregated spontaneously in a two-cluster structure as shown in Fig. 14. The two aggregates interact extremely weakly, and end by forming one connected cluster after a very long while. The occurrence of such disconnected atomic structures originates in the separable nature of the interaction (3) with respect to the ionic positions.

Some of the peculiar nanostructures described above may be stabilized either by geometric constraints (as, for instance, depositing them on surfaces, as we shall see in the next section), or by dynamic constraints. Indeed, we may apply a tension for instance on the two end-atoms of, say, the perfect 13-atoms icosahedron (or more complex structures), as produced by two forces acting in opposite directions, and look for equilibrium forms of such a distorted cluster. It is found that there are several discrete equilibrium forms up to breaking off the cluster, and the transverse size of the cluster is successively diminished in steps on increasing the applied force. These steps are very close to ”atomic steps”, corresponding to one atom getting in-line with the rest along the applied force, suggesting an ”atomic quantization” of the cross-section of the sample.

5. Metallic clusters deposited on surfaces

The summation over ionic positions in the potential energy (3) can be restricted to certain space regions, for instance to a half-space corresponding to a semi-infinite solid with a free, plane surface at x = 0. In this case we may use the continuum approximation, i.e. we may replace the summation over ionic positions in (3) by integration. We apply this procedure first to the self-consistent potential φ given by (2) and obtain:

$$\varphi(x) = \frac{4\pi z^*}{q^2 a^3}(1 - \frac{1}{2}e^{qx}) \ , \ x < 0 \ ,$$
$$\varphi(x) = \frac{2\pi z^*}{q^2 a^3}e^{-qx} \ , \ x > 0 \ , \qquad (5)$$

where z* is the average effective charge and a denotes the average inter-ionic distance; as mentioned in Section 2 we may take a ~2.73/q and $q \approx 0.77 z^{*1/3}$, as for a metal. Comparing the self-consistent potential (5) with the bulk contribution $\varphi = 4\pi z^*/q^2 a^3$ (obtained from (2) by integrating over the entire space), one can see that the surface brings its own contribution $\delta\varphi(x) = (2\pi z^*/q^2 a^3)(x/|x|)e^{-q|x|}$

to the self-consistent potential, which, through the selfconsistency relationship n = (q2/4_)', entails a spill δn of the electrons over the surface and a charge double layer at the surface, as expected. The total charge distribution at the surface double layer is shown schematically in Fig.15.

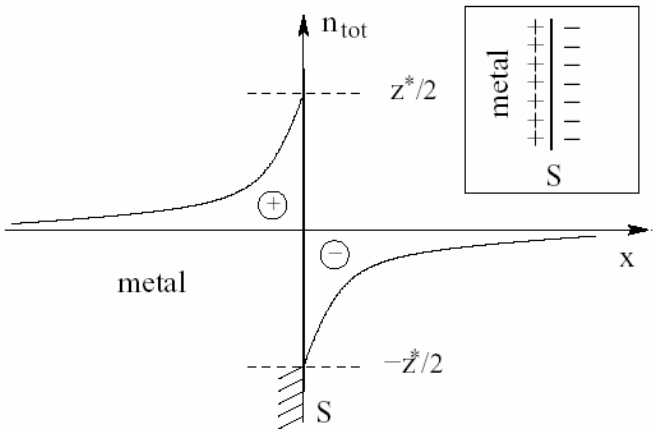

Figure 15 Charge distribution at the metallic surface double layer

The work function of the solid can be computed from (5), obtaining $\varphi = 4\pi z^*/q^2a^3$, as expected. The interaction energy $-(1/2)\ dx\cdot\delta\varphi\delta n$ associated with the electron double layer is $-\pi z^{*2}/2q^3a^6$ (per unit area), and it acts like an additional uncertainty in the quasi-particle energy, giving rise to boundary (finite-size) lifetime. It leads also to a weak relaxation of the ionic positions at the surface, which, however, is beyond the accuracy of the present computations. On the other hand, the potential energy (3) can be estimated for a semi-infinite metal in the continuum approximation, leading to

$$E_{pot} = -\frac{3}{4}qz^{*2}N + \frac{\pi z^{*2}}{2q^3a^6}A \ , \qquad (6)$$

where the first term is the bulk contribution (N represents the number of ions in metal), while the second term is the surface contribution, A denoting the area of the cross-section; hence, one may derive the surface tension $\sigma = \pi z^{*2}/2q^3a^6$ of a metal; it agrees with the energy given above for the electron double layer.

Similarly, by using (3) and (4), we can estimate the interaction potential between a semi-infinite metal and a metallic ion with an effective charge z^*_0 placed at distance *x* from the surface. We obtain

$$E_{pot} = E_s - \frac{3}{4}qz_0^{*2} - \frac{\pi z^* z_0^*}{qa^3}xe^{-q|x|} \ , \qquad (7)$$

where E_s denotes the potential energy of the solid as given by (6). One can notice in (7) the self-energy of the added ion and the last term which represents the solid-ion interaction potential.

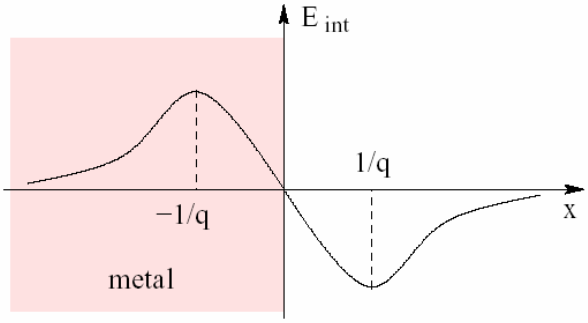

Figure 16 Interaction potential of a metallic ion and of a semi-infinite metal

This potential has an attractive tail above the surface and a repulsive barrier beneath, as shown in Fig. 16. The attractive part is responsible for forming up clusters added to the surface, while the interplay between the attractive and repulsive parts may determine the penetration of added atoms just beneath the surface, leading to diffusion and interfaces between a solid and a deposited cluster. It is worth noting that this interaction potential varies over a scale distance ~ 1/q, which is smaller than the average inter-ionic distance a ~ 2.73/q.

It is easy now, by making use of (7), to write down the potential energy of an ensemble of N metallic ions with effective charges z^*_i deposited on a metallic surface; it reads

$$E_{pot} = E_s - \frac{3}{4}q\sum_{i=1}^{N} z_i^{*2} + \frac{1}{2}\sum_{i\neq j=1}^{N} \Phi(R_{ij}) - \frac{\pi z^*}{qa^3}\sum_{i=1}^{N} z_i^* X_i e^{-q|X_i|} \quad , \tag{8}$$

where the potentials Φ(Rij) are given by (4) and X_i denotes the x-coordinate of $\mathbf{R}_i$. It is worth noting that the screening wave vector q in (8) is the one of the solid, as the latter prevails upon the deposited cluster in the thermodynamic limit. In this respect, the deposited clusters differ from isolated clusters which have their own screening wave vector, as resulting from the minimization of their quasi-classical energy. According to the theoretical approach presented in Section 2, the quasi-classical energy of the deposited cluster is $E_q = (27\pi^2/640)q^4\Sigma_i z^*_i + E_{pot} - E_s$, and the binding energy is $E = E_q - (9/32)q^2\Sigma_i z^*_i$. One can see here the separability of the general theoretical expression for the potential energy as given by (3) and (4) with respect to the ionic positions. We may also define an interaction energy from (8), between solid and a deposited cluster, by

$$E_{int} = -\frac{\pi z^*}{qa^3}\sum_{i=1}^{N} z_i^* X_i e^{-q|X_i|} \quad , \tag{9}$$

which may serve as a measure of the energy needed to separate the cluster off the surface (the difference in the cluster energy must be added, arising from its own screening wave vector corresponding to cluster relaxation). One can also check that the interaction energy (8) for the halves of a solid compensates exactly the surface energies of the two facets, as given by (6), as expected.

The main problem of depositing clusters on surface is the minimization of the potential energy given by (8) with respect to the ionic positions $\mathbf{R}_i$ (in fact, with respect to the reduced positions $q\mathbf{R}_i$). We follow the same procedure employed for isolated clusters, as described in Section 3, and illustrate the results here for Fe-clusters (z* = 0.57) deposited on Na surface (z* = 0.44). The ground-state mass spectrum for such clusters is shown in Fig. 17, up to N = 100. One can notice magic clusters deposited on surface like, for instance, those corresponding to N = 7, 14, 19, 23, 75, 77, 85, 88, 94... They may acquire highly symmetric forms as those shown in Figure 18.

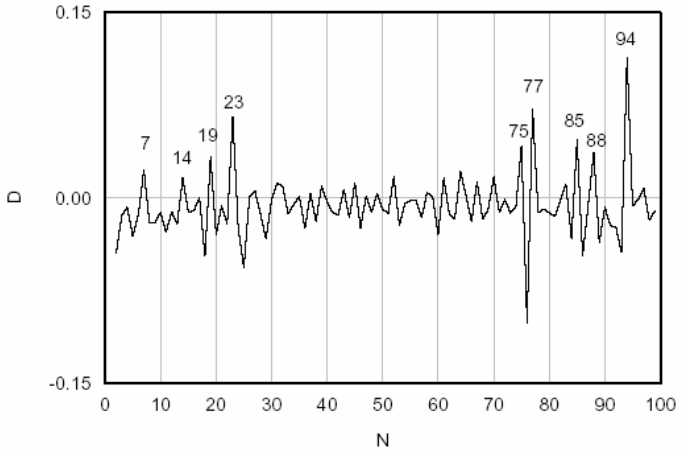

Figure 17 Ground-state mass spectrum of Fe-clusters deposited on Na-surface

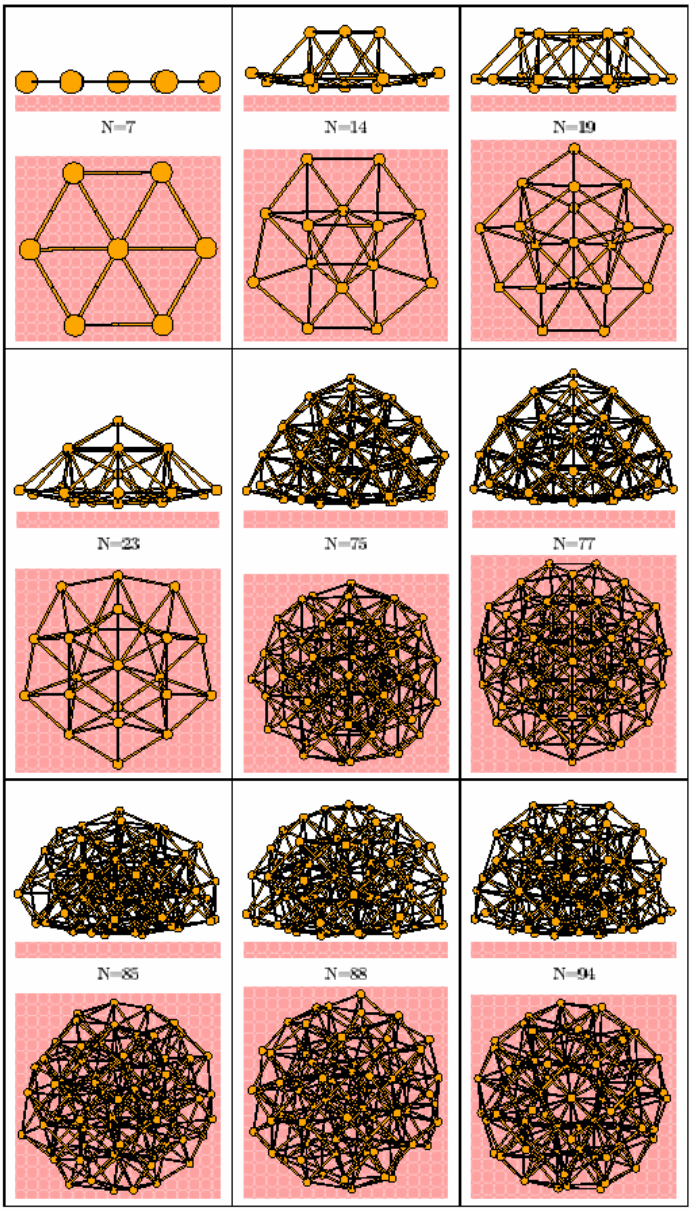

Figure 18 Magic Fe-clusters deposited on Na-surface: front view (upper rows) and top view (lower rows).

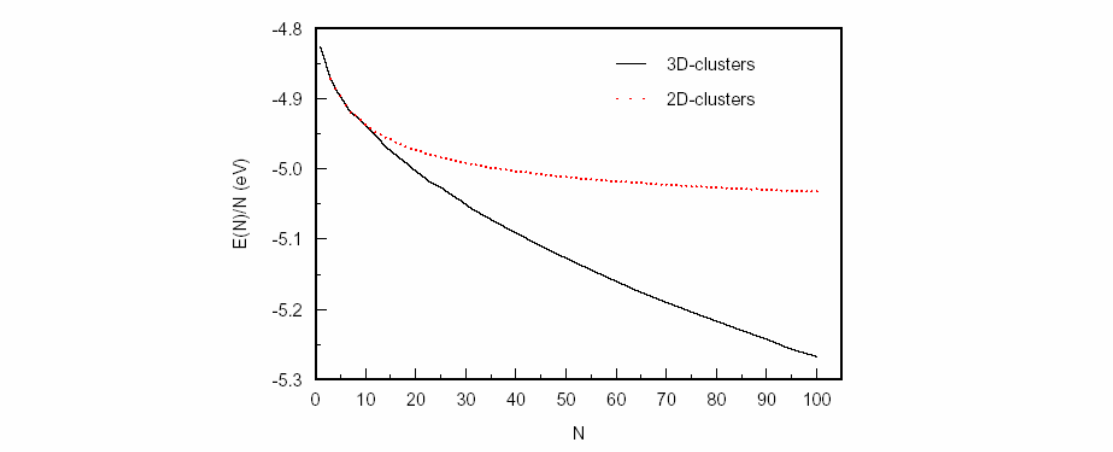

Figure 19 Ground-state energy per atom for Fe-clusters (3D, solid line) deposited on Na-surface *vs* cluster size, compared with monolayer cluster energy (2D, dashed line).

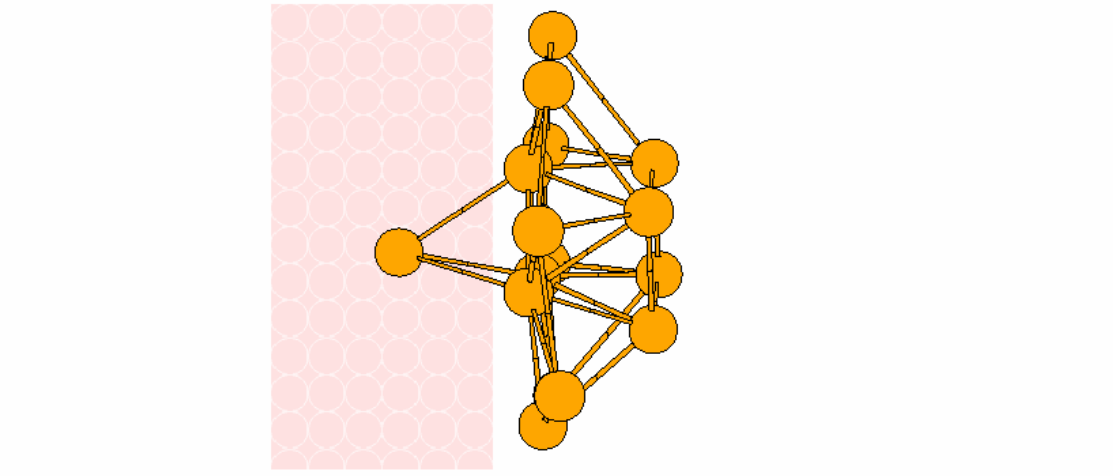

Figure 20 A deposited cluster with one ion beneath the surface.

The principle of their packing seems to be the same ”space economy”. For small values of N they arrange in rather regular polygons onto the surface, but with increasing N they start to construct up vertically, by adding successively multiple terraces, more or less regular; the overall constructions exhibit often a wonderfully intricate geometry, as one can see in Fig. 18 for N = 23, 77, 94, suggesting hats, theaters, stadium, domes, etc. In general, there is a competition between growing up vertically and lying down horizontally along the surface. We obtain monolayers (2D clusters) as ground-states for $N \leq 7$ and as isomers for $N > 7$, as shown in Fig. 19, where their binding energy is compared with the ground-state energy of deposited clusters (3D). We obtain also isomers, as expected, some of them with strange constructions close to instability (i.e. with high energies). There are many curiosities in constructing such deposited clusters, as for instance, the rather structureless island between N = 23 and N = 75 in Fig. 17, which is intriguing.

Some of the constructions obtained here theoretically can be found in experimental works.[16] In this connection it is worth noting that the continuum approximation employed here is, in fact, unnecessary, though useful; it affects the proximity properties between clusters and surface, and, of course, the problem of the ”lattice constants” matching.

Finally, it is worth presenting a very interesting situation shown in Fig. 20, where one added ion has penetrated beneath the surface, the rest having remained at the surface and formed there a

deposited cluster. The ion goes through the potential barrier shown in Fig. 16, and is kept

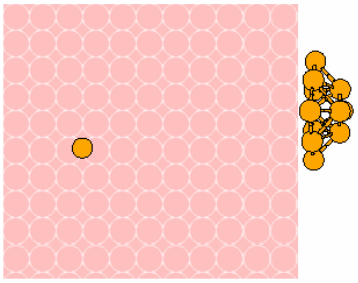

Figure 21 An ion diffused into solid from a deposited cluster.

in equilibrium by the interplay between the metal attraction and the surface-cluster attraction, which act in opposite directions. Such a cluster exhibiting an incipient interface with the solid is always an isomer, i.e. its energy is higher than the ground-state energy of a cluster of the same size deposited on surface. There appears also the possibility of a penetrating ion to escape into the solid, as shown in Fig. 21, where the position of the ion in solid is practically undefined, i.e. this ion is free; it has diffused into the solid. A more sizeable number of atoms may penetrate beneath the surface, as shown in the first two pictures in Fig.22 for a 50-atoms cluster, or for a 100-atoms cluster which developed a well-defined incipient interface with the solid (last picture in Fig. 22). These formations are incipient quantum dots of a very small size. Such results are encouraging for applying the present theoretical approach to more complex situations, in particular to nanostructures exhibiting interfaces, or other geometric and dynamic particularities.

6. Concluding remarks

The theoretical approach presented here deals with matter aggregation at the atomic level. It is based on the quasi-classical solution to Hartree-Fock equations describing a neutral ensemble of Coulomb interacting ions and valence electrons. The main ingredient of the theory is an inter-ionic effective (pseudo-) potential, of the type given by (4) for point-like effective ionic charges. The model has been applied to several species of metallic ions, leading to formation of homo-atomic clusters, either isolated or deposited on surfaces, as well as to some peculiar nanostructures, both with geometric and dynamic constraints. It provides quantitative results for geometric forms, ionic positions, inter-ionic distances, binding energies, both of ground-states and isomers, clusters stability and vibration spectra. Magic clusters and magic numbers have been obtained for ground states, giving an insight into the geometric patterns of cluster aggregation. At this level, the theoretical approach has a first-step approximation character, the full treatment requiring the so called quantum corrections. These provide single-particle properties, like electron energy levels, ionization potentials, chemical affinities, as well as response to external fields, transport and various spectroscopic properties included. The quantum corrections set also the ground for treating the clusters magnetism. The latter originates mainly in the electron ferromagnetism, as caused by the exchange interaction, and the ionic paramagnetism; both are to be treated in the particular context of a single-domain (or a few domains) magnetism, and a fractional occupancy of the electron levels, as required by the effective charge parameters. Both localized and itinerant magnetic moments are specific to clusters magnetism, with particular properties, like high, inhomogeneous magnetization, super-paramagnetism, etc. In addition, the model must be further refined by taking into account the spatial structure of the ionic charge distribution, in particular its angular dependence in oriented chemical bonds. This would considerably enlarge the applicability of the theory to large classes of chemical species.

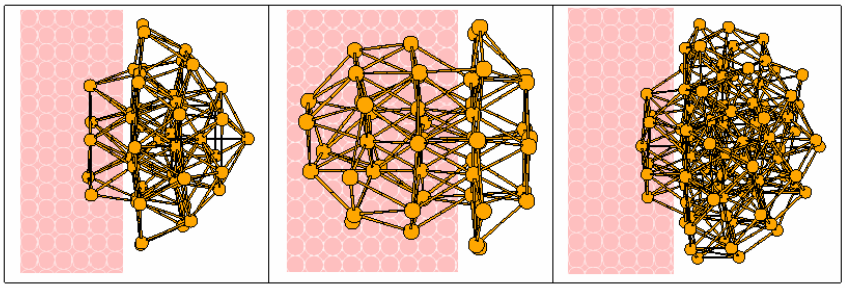

Figure 22: A 50-atoms cluster diffusing beneath a solid surface (first two pictures), and a 100-atoms cluster developing an incipient interface with a solid (last picture in the row)

Acknowledgments

This work has been partially supported by the Romanian Government CERES Research Programme #65/2001 and the Swiss National Science Foundation SCOPES Programme, Grant #7BUPJ062407.00/1-FCST.

References

[1] M. Apostol, J. Theor. Phys. 55, 82 (2000); ibid, 60 125 (2000).
[2] See, for instance, J. A. Pople, Revs. Mod. Phys. 71 1267 (1998) for a review.
[3] L. C. Cune and M. Apostol, Phys. Lett. A273 117 (2000); see also, L. C. Cune and M. Apostol, Metallic Binding, apoma, MB (2000).
[4] See, for instance, W. Kohn, Revs. Mod. Phys. 71 1253 (1998).
[5] J. C. Slater, Quantum Theory of Atomic Structure, McGraw-Hill, NY (1960).
[6] E. Wigner and F. Seitz, Phys. Rev. 43 804 (1934); ibid, 46 509 (1934); E. Wigner, Phys. Rev. **46** 1002 (1934); Trans. Faraday Soc. 34 678 (1938).
[7] J. C. Slater, The Calculations of Molecular Orbitals, Wiley, NY (1979).
[8] See in this context the "no-binding" theorem in E. Lieb and B. Simon, Adv. Math. 23 22 (1977), and L. Spruch, Revs. Mod. Phys. 63 151 (1991).
[9] J. Schwinger, Phys. Rev. A24 2353 (1981); see also ibid, A22 1827 (1980).
[10] Second reference cited under Ref. 3.
[11] See, for instance, J. P. K. Doye and D. J. Wales, J. Chem. Soc. Faraday Trans. 93 4233 (1997); W. A. de Heer, Revs. Mod. Phys. 65 611 (1993), M. Brack, Revs. Mod. Phys. 65 677 (1993) and references therein; D. Rayane, P. Melinon, B. Tribollet, B. Chabaud, A. Hoareau and M. Broyer, J. Chem. Phys. 91 3100 (1990).
[12] B. I. Dunlap, Phys.Rev. A41 5691 (1990); M. Castro and D. R. Salahub, Phys. Rev. B47 10 955 (1993); O. B. Christensen and M. L. Cohen, ibid, B47 13 643 (1993); Q. Wang, Q. Sun, M. Sakurai, J. Z. Yu, B. L. Gu, K. Sumiyama and Y. Kawazoe, Phys. Rev. B59 12 672 (1999).
[13] V. Bonacic-Koutecki, P. Fantucci and J. Koutecki, Phys. Rev. B37 4369 (1988); J. Chem. Phys. 93 3802 (1990); Chem. Rev. 91 1035 (1991); P. Ballone, W. Andreoni, R. Car and M. Parinello, Europhys. Lett. 8 73 (1989); W. Andreoni, Z. Phys. D19 31 (1991); U. Rothlisberger and W. Andreoni, J. Chem. Phys. 94 8129 (1991); W. A. de Heer, W. D. Knight, M. Y. Chou and M. L. Cohen, in H. Ehrenreich and D. Turnbull (eds), Solid State Physics, Academic, NY (1987), vol. 40, p. 93; C. Brechignac, P. Cahuzac, F. Carlier, M. de Frutos and J. Leygnier, Chem. Phys. Lett. 186 28 (1992); C. Brechignac, P. Cahuzac, M. de Frutos, J. P. Roux and K. H. Bowen, in P. Jena et al (eds), Physics and Chemistry of Finite Systems: From Clusters to Crystals, Kluwer, Academic, Dordercht (1992), vol. 1, p. 369.
[14] F. Huisken , B. Kohn, R. Alexandrescu and I. Morjan, J. Chem. Phys. 113 6579 (2000).
[15] L. C. Cune and M. Apostol, Chem. Phys. Lett. 344 287 (2001).
[16] See, for instance, K.-H. Meiwes-Broer (ed), Metal Clusters at Surfaces: Structure, Quantum Properties, Physical Chemistry (Cluster Physics), Springer (2000).